Neoplasia • Vol. 1, No. 5, November 1999, pp. 438–445 438

Available On-line at http://www.neoplasia.org

Treatment of Experimental Brain Tumors with Trombospondin-1 Derived Peptides: an *In Vivo* Imaging Study

A. Bogdanov, Jr.[*1], E. Marecos*[*1], H.C. Cheng*[†], L. Chandrasekaran*[‡], H.C. Krutzsch*[‡], D.D. Roberts*[‡] and R. Weissleder**

*Center for Molecular Imaging Research, Massachusetts General Hospital, Bldg. 149, 13th St., Charlestown, MA 02129; [†]Taiwan Veterans Administration Hospital, Taipei, Taiwan; [‡]Laboratory of Pathology, National Cancer Institute, National Institutes of Health, Bethesda, MD 20892-1500

Abstract

Antiangiogenic and antiproliferative effects of synthetic D-reverse peptides derived from the type 1 repeats of thrombospondin (TSP1) [1,2] were studied in rodent C6 glioma and 9L gliosarcomas. To directly measure tumor size and vascular parameters, we employed *in vivo* magnetic resonance (MR) imaging and corroborated results by traditional morphometric tissue analysis. Rats bearing either C6 or 9L tumors were treated with TSP1-derived peptide (D-reverse amKRFKQDGGWSHWSPWSSac, $n=13$) or a control peptide (D-reverse amKRAKQAGGASHASPASSac, $n=12$) at 10 mg/kg, administered either intravenously or through subcutaneous miniosmotic pumps starting 10 days after tumor implantation. Eleven days later, the effect of peptide treatment was evaluated. TSP1 peptide-treated 9L tumors (50.7±44.2 mm^3, $n=7$) and C6 tumors (41.3±34.2 mm^3, $n=6$) were significantly smaller than tumors treated with control peptide (9L: 215.7±67.8 mm^3, $n=6$; C6: 184.2±105.2 mm^3, $n=6$). In contrast, the *in vivo* vascular volume fraction, the mean vascular area (determined by microscopy), and the microvascular density of tumors were not significantly different in any of the experimental groups. In cell culture, TSP1, and the amKRFKQDGGWSHWSPWSSac peptide showed antiproliferative effects against C6 with an IC of 45 nM for TSP1. These results indicate that TSP1-derived peptides retard brain tumor growth presumably as a result of slower *de novo* blood vessel formation and synergistic direct antiproliferative effects on tumor cells. We also show that *in vivo* MR imaging can be used to assess treatment efficacy of novel antiangiogenic drugs non-invasively, which has obvious implications for clinical trials.

Keywords: thrombospondin-1, magnetic resonance, imaging, peptide, anti-angiogenesis.

Introduction

Angiogenesis is implicated in the pathogenesis of tumor growth and metastasis (reviewed in [3–5]). Several studies have shown a correlation between high microvessel counts and a poor prognosis, poorer disease-free survival and or increased risk for metastasis, particularly in breast cancer [6,7]. These studies raise hope for improved cancer treatment strategies involving selective inhibition of tumor vascular endothelial proliferation [8,9] or targeted killing of vascular endothelial cells in tumors [10–12].

There has been recent interest in applying antiangiogenic strategies to treat brain tumors using different angiogenesis inhibitors. These studies have included gene transfer of vascular endothelial growth factor (VEGF) antisense cDNA [13–15], angiostatin [16,17] or gene transfer using angiostatin cDNA [18]. Additional angiogenesis inhibitors are under development, including peptides derived from the angiogenesis inhibitor TSP1 [19,20]. Several mechanisms may account for the antiangiogenic activity of thrombospondin-1 (TSP1). TSP1 inhibits the adhesion of endothelial cells to a fibronectin matrix [21], suggesting that the loss of adhesion may inhibit endothelial proliferation. TSP1 also inhibits growth and motility of endothelial cells stimulated by FGF-2 by directly inhibiting growth factor binding [22]. Furthermore, TSP1 overexpression suppresses tumor growth in several rodent xenograft models [23–26]. Several small peptide fragments isolated from central 70 kDa stalk region of the TSP1 molecule exhibit antiproliferative effects against endothelial cells [22,27]. The inhibition of cell proliferation is caused by activity associated with the two domains of the central stalk, the procollagen homology region, and the properdin-like type 1 repeats [22,27]. This activity of TSP1 is also mimicked by the synthetic peptides derived from the type 1 repeats of TSP1 [1,2] that were used in the current study.

The current study was conducted to evaluate the effect of a model TSP1-derived peptide on the growth of different rodent gliomas. The synthetic peptide analog derived from the TSP1 was D-reverse amKRFKQDGGWSHWSPWSSac.

Address all correspondence to: Dr. A. Bogdanov, Jr., Center for Molecular Imaging Research, Rm. 5420, Massachusetts General Hospital, Bldg. 149, 13th Street, Charlestown, MA 02129.

[1] These authors contributed equally to this work.

Received 27 May 1999; Accepted 26 July 1999.

The peptide was administered to rodents bearing intracranial C6 glioma (expressing *lac Z* as a marker) or 9L gliosarcomas (expressing GFP as a marker) 10 days after stereotactic tumor implantation. *In vivo*, postmortem and *in vitro* studies were conducted to answer the following questions: (1) Is the TSP1-derived peptide active against rodent gliomas?; (2) Does a potential antitumor effect occur solely through antiangiogenic effects as previously demonstrated or also synergistic antitumoral effects?; (3) What is the effect of peptide treatment on tumor size and functional vascular parameters during tumor growth?; and (4) Can *in vivo* magnetic resonance (MR) imaging be used to predict antiangiogenic effects observed during the traditional morphometric evaluation?

Materials and methods

Cell Culture

Rat 9L-GFP-34-1 gliosarcoma cells [28] and BAG C6 rat glioma cells (ATCC) were grown in Dulbecco's modified Eagle's medium (DMEM, Cellgro, Mediatech, Washington, D.C.) with 10% fetal bovine serum (FBS, Cellgro) and 1% penicillin/streptomycin (Cellgro), 37°C in 5.5% CO_2 with medium change every 3 to 5 days.

Anti-angiogenic Peptides

A synthetic D-inverse peptide analog derived from the type 1 repeats of human TSP1 D-reverse amKRFKQDGGWSH-WSPWSSac (P1) was synthesized and characterized as previously described [1,2]. This peptide was used for all *in vivo* studies. Peptide sequences were also synthesized containing appropriate Ala substitutions to eliminate the essential Phe residue for latent transforming growth factor (TGF) activation (D-reverse amKRAKQAGGWSHWSPWSSac, P2) and the Trp residues required for heparin binding (D-reverse amKRAKQAGGASHASPASSac, P3, control peptide). Peptides were dialyzed using 500 MWt cutoff tubing (Spectrapor) and stored in lyophilized form. Ficoll conjugates of the peptides [1,2] were also used for some *in vitro* analyses of glioma cell proliferation. To study the blood half-life and biodistribution, P1 was radioiodinated by incubating 100 μg of peptide at 1 mg/ml with 500 μCi of carrier-free $Na^{125}I$ in the presence of 20 μg of Iodogen (Pierce, Rockford, IL). The peptide was purified from unincorporated iodine by Biogel P-2 column chromatography using 10 mM sodium citrate, 0.15 M NaCl, pH 7 as eluant. The radiochemical purity of labeled P2 was confirmed using thin-layer chromatography (Kieselgel 60 F_{254}; eluted with butanol: acetic acid:water 3:2:1). To study the intratumoral distribution, we also fluorescently labeled the P1. This was accomplished by incubating the peptide with rhodamine-X-isothiocyanate at a molar ratio of 1:3 in 0.1 sodium carbonate, pH 10 for 1 hour. The solution was treated with 0.1 M hydroxylamine and the conjugate was purified using chromatography on BioGel P-2 as described above.

Anti-Proliferative Properties of TSP1 in C6 Cells

To study potential direct antiproliferative effects of TSP1-derived peptide on C6 cells, the following experiments were performed. A 100 μl suspension of C6 glioma cells at a concentration of 50,000 cells/ml in DMEM containing 1% FBS were plated in triplicate in 96-well tissue culture plates in the presence of inhibitors, including TSP1, Ficoll-conjugated and free peptides. TSP1 was used in solution at concentrations ranging from 5 nM to 44 nM. Conjugated peptides were used in solution at concentrations of 0.63 to 2.5 μM and free peptides were used in concentrations from 0.04 μM to 50 μM. Cells were grown for 72 hours at 37°C in a humidified incubator with 5% CO_2. Proliferation was determined as previously described [22].

Biodistribution and Blood Half-Life Determination

Female Fischer rats (n=3/group) were anesthetized using 65 mg/kg sodium pentobarbital and TSP1-derived peptide was injected intravenously at 10 mg/kg in 500 μl sterile saline containing 12.5 μCi ^{125}I-labeled peptide/dose. Blood samples were withdrawn from the contralateral tail vein at several time intervals. At 1, 2, and 24 hours, animals were sacrificed by sodium pentobarbital overdose, and the tumor and major organs were excised, weighed, and radioactivity was determined by gamma-counting. Blood volume correction was performed as described before [29].

9L-GFP, C6 Models and Experimental Treatment

A total of 25 female Fischer 344 rats weighing between 180 and 190 g (Charles River Breeding Laboratories, NC) were used for 9L-GFP-34-1 rat gliosarcoma cells (n=13) or C6 rat glioma cells (n=12) intracerebral implantation. To induce tumors, animals were anesthetized as above and immobilized in a stereotactic frame (David Kopf Instruments, Tujunga, CA). Approximately 1 mln cells in 10 μl of Hanks' balanced salt solution (HBSS; Cellgro) were injected into the putamen at a depth of 3.5 mm from the dural surface. The injection was made over 5 minutes, and the needle was withdrawn slowly over another 5 minutes. The animal protocol was approved by the Institutional Review Committee on Animal Care and was conducted in accordance with National Animal Welfare guidelines. Treatment with peptides was initiated 10 days after implantation of tumors at which point the tumors were approximately 60±5 mm^3 in size. Animals were divided into two groups: (a) was treated with TSP1-derived peptide P1, and (b) with control peptide. Peptides were administered intravenously at the dose of 10 mg/kg (four doses every second day). Higher doses of peptides (20 mg/kg) resulted in pronounced toxicity. In some animals, the same amount of the peptide was delivered using Alzet-2002 miniosmotic pumps (0.5 ml/h; 7.5 mg of peptide delivered continuously for 10 days, n=6). The pumps were implanted subcutaneously in the neck. No adverse effects were observed due to this mode of delivery. MR imaging was performed in both control and experimental groups 21 days after implantation.

Paramagnetic MR Imaging Probes

The paramagnetic probe used to delineate the vascular space for *in vivo* MR imaging was a previously developed and characterized synthetic graft copolymer. The agent was synthesized by covalent modification of (*O*-methyl poly (ethylene glycol)-*O′*-succinyl-*N*-*O′*-poly(L-lysine), MPEGs-PL graft co-polymer with DTPA cyclic anhydride as described in Refs. [29,30]. The product was purified by ultrafiltration using an UFP-300 cartridge (A/G Technology Co.). The duration of ultrafiltration was determined by size-exclusion high-performance liquid chromatography (HPLC) analysis (Hydropore-5-SEC, 4.5 mm ID×25 cm L, Rainin Instr. Co., Woburn, MA) eluted with 50 mM sodium phosphate, pH 6.8, at 0.5 ml/min. Composition of the co-polymer was confirmed by elemental analysis (Galbraith, Labs, Knoxville, TN). The molecular mass of MPEG-PL was calculated as 410 kDa. The pharmacokinetic behavior of MPEG-PL-DTPA(Gd) has been evaluated in more detail elsewhere [31]. The agent has a blood half-life of 36 hours (at 5 to 50 μmol Gd/kg body weight, in rats). An interstitial contrast agent, gadodiamide (Omniscan, Nycomed, New York, NY) was obtained commercially and used to enhance the tumor for tumor volume measurements.

MR Imaging

MR imaging was performed on a 1.5 T superconducting magnet (Signa 5.0; GE Medical Systems, Milwaukee, WI) using a 3-inch surface coil. The imaging protocol (that was optimized as reported in [32]) consisted of an axial 3D Fast Spoiled Gradient Recalled sequence (fast SPGR) with a TR/TE of 26.1 ms/min and a flip angle of 30°, 10 cm field of view, 256×160 matrix size with 1 NEX and 12 sections (1 mm section thickness). Three acquisitions were performed before, and five acquisitions after the administration of MPEG-PL-DTPA(Gd) followed by five acquisitions after the injection of gadodiamide. The total amount of gadolinium bound to MPEG-PL-DTPA was 90 μmol Gd/kg resulting in blood T1 relaxation times of <50 msec [31,33]. A dose of gadodiamide (200 μmol Gd/kg) was injected at the end of the study to better delineate the tumor. The total scan time including a localizer sequence (2D fast SPGR, with a TR of 150 ms, a TE of 2.1 ms, and a flip angle of 30°) was less than 20 minutes.

Image analysis was performed as in [32]. For each animal, all tumor-containing imaging slices were analyzed. The criterion for inclusion of the image in analysis was positive enhancement with gadodiamide. Since MPEG-PL-DTPA-Gd does not leak into the interstitial space during the time course of the study (15 minutes), the fractional flux rate from the capillaries into the interstitium was assumed to be negligible [31,34]. Therefore, rVVF (relative vascular volume fraction) of tumor scaled to that of the contralateral normal brain was defined as the ratio of $\Delta SI_{tumor}/\Delta SI_{contralateral\ normal\ brain}$, where ΔSI is the change in signal intensity after MPEG-PL-DTPA-Gd injection [32]. Average images of precontrast (n=3) and postcontrast (n=5) images were obtained and subtracted (postcontrast minus precontrast) on a pixel by pixel basis. Signal intensity measurements were determined in regions of interest (ROI), such as tumor and contralateral normal brain. To characterize local heterogeneity of rVVF, we also sorted individual pixels corresponding to the tumor region into three categories. Pixels with ΔSI_{tumor} that was higher than the median $\Delta SI_{contralateral\ normal\ brain} + 2SD$ (standard deviation) were assigned to the hypervascular fraction of tumor. Pixels corresponding to $\Delta SI_{contralateral\ normal\ brain} \pm 2SD$ were labeled as isovascular fraction, and pixels with ΔSI_{tumor} lower than the median of $\Delta SI_{contralateral\ normal\ brain}$-2SD corresponded to the hypovascular fraction of the tumor. Therefore, all fractions were scaled to that of the ΔSI of the contralateral normal brain tissue. For MR tumor size measurements, voxel size was calculated as follows: voxel size = $(F/m)*(F/n)*l = 0.24347\ mm^3$, where F=100 mm (field of view); $m*n$ = 256×160 (matrix size) and l = 1 mm (slice thickness). Tumor volume was calculated as the total number of pixels (in all slices that contain tumor) multiplied by a voxel size.

Histology

Immediately after imaging, animals were sacrificed by pentobarbital overdose. Tissues were treated with 2% formaldehyde in phosphate-buffered saline (PBS), pH 7.5 followed by 30% sucrose solution. Some control animals were injected intravenously with 0.5 ml of 0.2% Hoechst 33258 dye [35] in saline (Molecular Probes, Eugene, OR) and immediately sacrificed with an overdose of pentobarbital, followed by perfusion with 250 ml of phosphate-buffered 4% formaldehyde. Tumor samples equilibrated in sucrose were positioned for cutting into equatorial sections as described in [36,37], frozen and cut into 8 μm sections. Immediately after sectioning, fluorescence microscopy was performed using an inverted microscope (Zeiss Axiovert 100 TV, Wetzlar, Germany) fitted with a DAPI and fluorescein filter sets (Omega Optical, Brattleboro, VT). Images were acquired using a Photometrics CH250 cooled CCD (Photometrics, Tucson, AZ) with image acquisition and storage controlled by IP LabSpectrum software (Signal Analytics, Vienna, VA).

Parallel sections were fixed in 2% formaldehyde/PBS and incubated with mouse anti-rat CD-31 antibody diluted 1:1000 (Serotec, Oxford, UK) followed by incubation with biotinylated secondary antibody diluted at 1:5000 (goat anti-mouse; Pierce, Rockford, IL) and avidin–peroxidase complex (Vector Laboratories, Burlingame, CA) as suggested by the manufacturer. After incubating with DAB/H_20_2, sections were dehydrated and counterstained with Gill's #1 hematoxylin (Fisher Scientific, Fair Lawn, NJ).

Microvascular Density

Microvessel density (MVD) was counted by using two different approaches: (1) by counting non-fluorescent ("black spots") on digitized fluorescent images of the tumor (black spots represent tumor vessels [28]), and (2) by counting CD31-positive vessels. In all cases, MVD was determined in areas of visually dense neovascularization ("hot spots") as described in [6,38,39]. Three hot spots were identified within four 8-μm thick sections for each of

the animals by both methods. Results were expressed as the mean number of microvessels identified within any single area 1 mm^2 and as a fraction of the total tumor area, at a magnification of ×100. The fraction of tumor area occupied by blood vessels in sections was considered to be the estimate of the total tumor vascular volume as suggested in [36].

Statistical Analysis

Data analysis was performed using the unpaired two-tailed *t*-test with Welch's correction. Statistical significance was assigned for *p* values of less than 0.05. Non-linear regression modeling and analysis of blood elimination data was accomplished using Prism 2 software (GraphPad Software).

Results

In Vitro Proliferation

To determine whether different peptides had direct antitumor effects in addition to known antiangiogenic effects, we performed proliferation assays using the C6 glioma cell line (Figure 1). Intact TSP1 inhibited proliferation with an IC_{50}=45 nM. This is 6- to 15-fold weaker than the antiproliferative activity of TSP1 for endothelial cells (IC_{50}=7 nM, corneal endothelial [22], IC_{50}=3 nM, aortic endothelial [2]). As previously reported for melanoma and endothelial cells *in vitro* [1,2], Ficoll conjugates were more potent inhibitors of C6 glioma cell proliferation than the corresponding free peptides. The Trp residues were required for inhibition of proliferation, because the control peptide D-reverse amKRAKQAGGASHASPASSac was inactive (Figure 1). However, the latent TGFβ-activating sequence was not required, since the peptides and Ficoll conjugates lacking this sequence had similar activities as the native TSP1 peptide sequence.

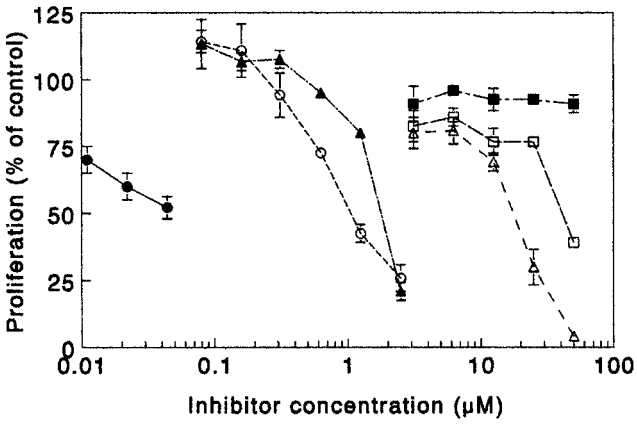

Figure 1. *C6 glioma cells (5000/well in DMEM containing 1% FBS) were plated in 96 well tissue culture plates in the presence of the indicated concentrations of human platelet TSP1 (closed circles), Ficoll-conjugated peptides D-reverse-amKRFKQDGGWSHWSPWSS-thiopropionyl-AECMficoll (open circles) and D-reverse-amKRAKQAGGWSHWSPWSSC-AECMficoll (closed triangle), and free peptides D-reverse-amKRAKQAGWSHWAAac (open triangle), D-reverse-amKRAKQAGGWSHWSPWSSac (open squares), and D-reverse-amKRAKQAGGASHASPASSac (filled squares). Cells were grown for 72 hours at 37°C in a humidified incubator with 5% CO_2. Proliferation was quantified using the Promega Celltiter assay. Results are presented as a percentage of control proliferation determined without inhibitors, mean±SD, n = 3.*

Table 1. Biodistribution of ^{125}I-labeled TSP1 derived peptide at 1 and 24 hours after the administration (10 mg peptide/kg). Data presented as mean ± SD (*n*=2–3).

Tissues and organs	Percentage dose/g tissue, 1 hour	Percentage dose/g tissue, 24 hours
Blood	0.23±0.11	0.15±0.06
Bone	0.13±0.03	0.01±0.00
Brain	0.002±0.001	0.0008±0.0003
Fat	0.008±0.008	0.002±0.001
Heart	0.21±0.10	0.12±0.03
Intestine	0.03±0.01	0.02±0.01
Kidney	0.30±0.09	0.21±0.10
Liver	2.55±0.76	1.35±0.54
Lung	0.38±0.21	0.05±0.03
Muscle	0.003±0.001	0.011±0.004
Spleen	0.15±0.03	0.18±0.07
Stomach	0.04±0.01	0.04±0.03
Tumor	0.035±0.002	0.012±0.006

Distribution and Fate of IV Injected Peptide

Radioiodinated, purified P1 was obtained at 98% radiochemical purity (by thin-layer chromatography, TLC) and used for biodistribution studies in 9L-gliosarcoma-bearing rats. Blood elimination data were used for two-compartmental (biexponential) modeling of clearance. There was a rapid clearance of the peptide from the bloodstream (95% initial dose, $t1/2$=0.056 hour, r^2=0.998) through kidneys with urine. A minor slower component (5% initial dose, $t1/2$=50.5 hours, r^2=0.98) was also identified. The P1 peptide accumulated primarily in liver and lung (Table 1). Tumor accumulation was 0.03% to 0.04% dose/g after 1 hour and showed a slow washout. The accumulation in normal brain tissue was approximately 20-fold lower than in tumors. Fluorescence microscopy of brain tumor slices, obtained from animals injected with Rhodamine-X-labeled peptide showed prominent fluorescence of the tumor endothelium and some labeling of interstitium (Figure 2, *A* and *B*). The binding of fluorescent-labeled peptide to the vessels was inhibited by a preinjection of tumor-bearing animals with a single dose of P1 (10 mg/kg) 20 minutes before injecting Rhodamine-X-labeled P1. The binding to normal brain microvessels was detectable, but much less prominent than in tumor (Figure 2*C*).

Effect of Peptides on Brain Tumor Growth

The treatment of C6 glioma and 9L gliosarcoma-bearing animals with peptides was conducted using two different approaches. To measure the tumor size, *in vivo* MR imaging was used (Figure 3). Quantitative image analysis showed that tumors in animals injected with the TSP1 peptide were significantly smaller compared to

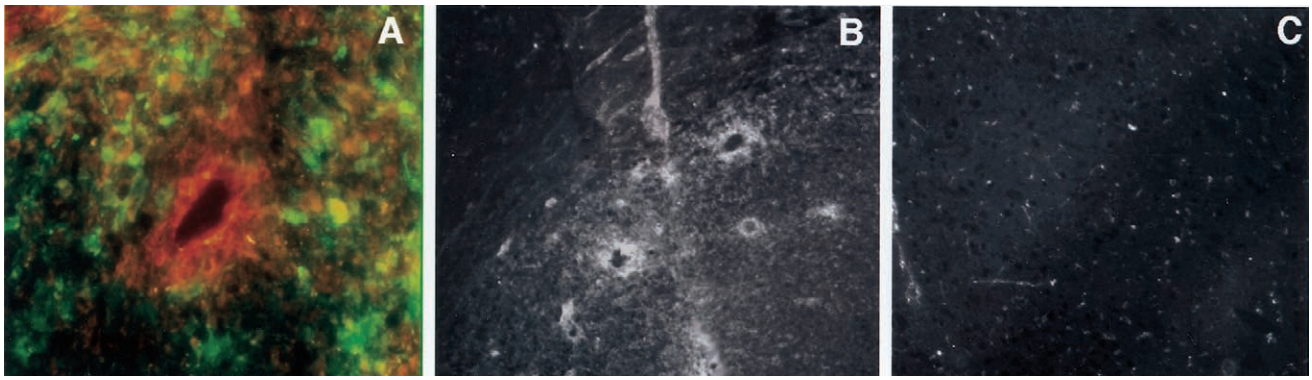

Figure 2. *Distribution of fluorescent-labeled TSP1 derived peptide in gliosarcoma and normal brain as determined by fluorescent microscopy of 9L-GFP-34-1 tumor sections (thickness – 8 μm). Tumors were implanted in the brain of Fischer rats stereotactically as described in Materials and Methods. Rhodamine-X-labeled P1 (rv-amKRAKQAGGWSHWSPWSSac) was injected IV at 10 mg/kg. Animals were sacrificed at 1 hour after administration of the peptide and brain tissue was processed for microscopy. (A) Dual channel microscopy of a blood vessel at the tumor/normal brain interface. Red — Rhodamine-X-peptide, green — GFP expressing 9L cells. Magnification 250×. (B) Distribution of Rhodamine-X-peptide in 9L tumor. Magnification, 60×. (C) Distribution of Rhodamine-X-peptide in contralateral normal brain. Magnification 60×.*

animals treated with the control peptide. The mean 9L tumor volumes (mean±SD) were as follows: 215.7±67.8 mm^3 for control (non-treated) animals and 50.7±44.2 mm^3 for P1-treated animals (p=.0008). Similar effects were observed in C6 glioma-treated and control animals; 184.2±105.2 mm^3 for control animals and 41.3±34.2 mm^3 for P1-treated animals (p=.0022). To determine the effects of the peptide treatment on vascular parameters of tumors, we used a previously described imaging method [32]. The relative vascular volume fraction (rVVF mean±SD) were as follows: 9L tumors, 1.89±0.21 (experimental) and 2.26±0.30 (control); C6 tumors, 2.10±0.20 and 2.01±0.20 experimental and control groups, respectively. The fractions of voxels within tumors that were assigned differential vascularity ranks based on SI (hyper-, iso-, and hypovascular, Table 2) were similar in P1-treated and control peptide-treated groups. As expected, the more vascular tumor periphery showed a higher rVVF and larger number of hypervascular voxels than the less vascular tumor center, but there was no statistically significant difference among the groups.

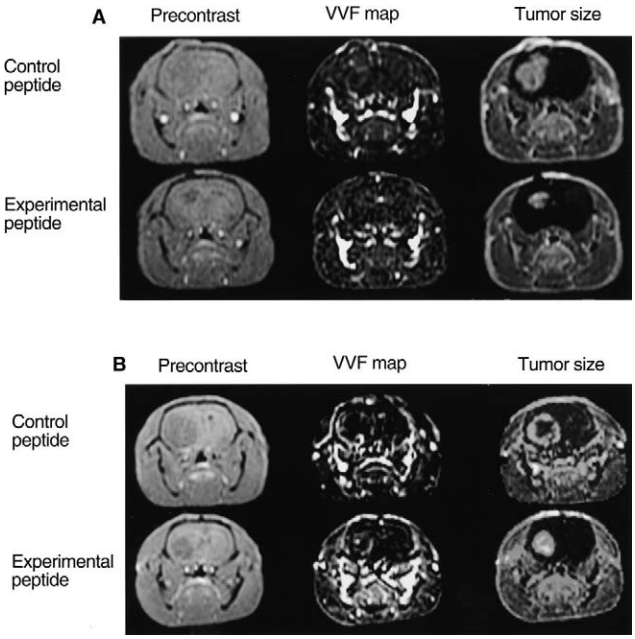

Figure 3. *Non-enhanced and contrast-enhanced representative MR axial maps of intracerebrally implanted tumors in animals treated with control and experimental (TSP1 derived peptide). (A) 9L-GFP-34-1 tumor. (B) C6 tumor.*

Microvascular Density

Table 2 summarizes the results from Microvascular Density counting. Microvascular Density (expressed as the mean number of vessels identified within any single tumor area 1 mm^2) in control tumors was 37 vessels/mm^2 similar to the density of 39 vessels/mm^2 in the P1-treated group. We also performed a section analysis based on fluorescence and non-fluorescence in 9L-GFP tumors as previously

Table 2. Magnetic resonance and histology characterization of experimental brain tumors in TSP1 derived peptide-treated and control animals.

	9L-GFP-34-1		C6	
	TSP1 derived	Control peptide	TSP1 derived	Control peptide
Tumor size (mm^3)	50.7±44.2	215.7±67.8	41.3±34.2	184.4±74.4
rVVF of tumor*	1.89±0.21	2.26±0.30	2.10±0.20	2.00±0.20
Vascularity†				
Hypovascular	5.1±2.1	5.2±4.0	4.9±4.0	5.3±3.3
Isovascular	61.7±18.1	53.3±7.1	58.9±14.2	65.8±9.9
Hypervascular	33.2±21.2	41.5±10.8	36.2±9.5	28.9±7.0
Vascular area fraction, %‡	5.06±1.76	5.58±1.81	ND	ND
Vessel count, per mm^2	39	37	ND	ND

*Scaled to VVF of the contralateral normal brain.
†Percentage compared to the contralateral normal brain ± 2SD.
‡Determined using fluorescent microscopy and anti-CD-31 as described in Materials and Methods.
ND=not determined.

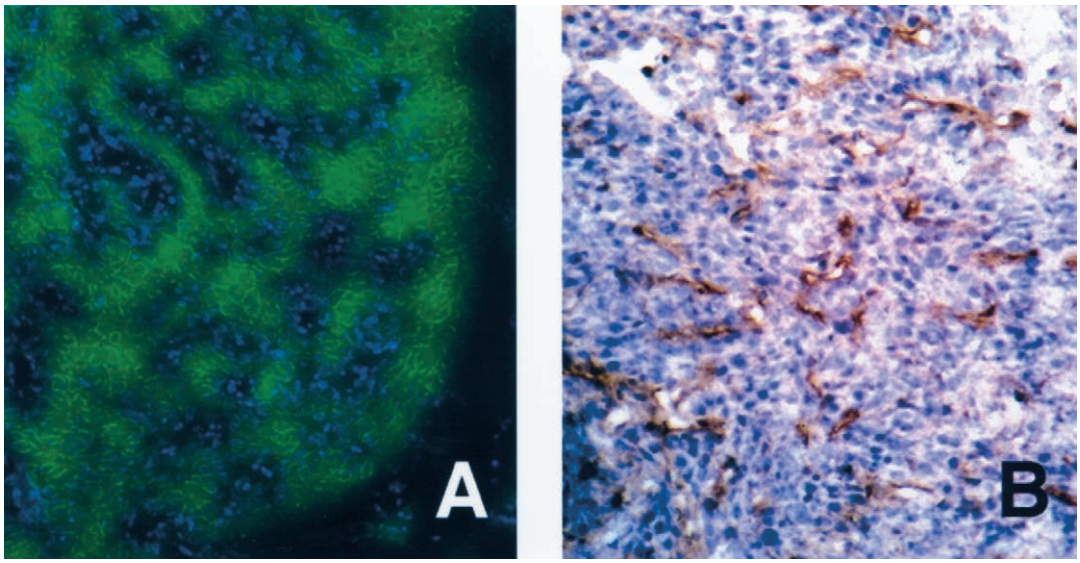

Figure 4. *Fluorescence microscopy and immunohistology of 9L-GFP-34-1 tumor sections (8 μm). Tumors were implanted in the brain of Fischer rats stereotactically as described in Materials and Methods. (A) Double-channel fluorescent microscopy of brain tissue isolated from rats that received injection of Hoechst dye immediately before euthanasia. Green — GFP; Blue — Hoechst. (B) Anti-CD31 immunohistology of a parallel section. Blood vessels are delineated using secondary antibody-peroxidase/DAB stain with subsequent counter staining with hematoxylin. Magnification 100×.*

described [28]. In all sections studied, there was a clear correlation between the non-fluorescent "black spots" distribution that was detected using fluorescence microscopy (Figure 4*A*) and blood vessel lining endothelium revealed by Hoechst staining (Figure 4*A*) or by anti-CD31 antibodies (Figure 4*B*). Quantitative image analysis showed the percentage of area occupied by blood vessels with respect to the total area examined to be as follows: 5.06±1.76% for the P1-treated group and 5.58±1.81% for the control tumors ($p=0.1954$). The distribution of blood vessel areas measured using digitized images of 9L-GFP tumor sections ($n=300$/each group) showed that there was a significant difference in mean blood vessel lumenal area: 1245±61 μm^2 in P1-treated vs. 1514±75 μm^2 in control tumors ($p=0.0051$; Figure 5). In addition, we observed a lower number of very large vessels (area >3000 μm^2) in treated tumors than in untreated tumors.

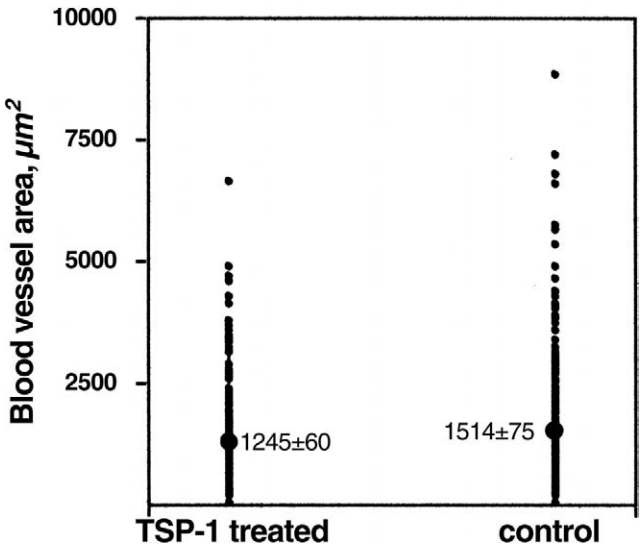

Figure 5. *Cross-sectional vessel area measured using fluorescent 9L-GFP-34-1 tumor section images. Sections were prepared from the animals treated with control and experimental peptides (n=300 in each data set). Numbers represent mean±SEM.*

Discussion

Antiangiogenic therapy has been shown to be efficient in inhibiting proliferation of many rodent tumors [8,9,40,41]. Because of the grave prognosis of malignant brain tumors, novel antiangiogenic therapies are under development [18]. The goal of this study was to investigate antiangiogenic effects of peptides derived from TSP1 using rodent gliomas as a model system. The involvement of TSP1 in regulation of angiogenesis in highly vascularized glioblastomas has been established before [25]. In the current study, we examined two brain tumor models, one of which has been recently described [28], both by *in vivo* MR imaging [32] and also by histological evaluation. Our data show that a TSP1-derived peptide P1 had a significant effect on glioma progression when compared to the relevant control peptide.

TSP1 is an extracellular matrix glycoprotein that has multiple effects on cell–matrix interactions and proliferation (reviewed in [42]). In many tumors [23–26], but with some notable exceptions [43,44], TSP1 expression inhibits both tumor growth and development of tumor blood vessels. Because of these effects, TSP1 was identified as a potential regulator of tumor growth and metastasis. TSP1 binds to

several cell-surface receptors, heparan sulfate proteoglycans, growth factors, and other components of extracellular matrix. The multiple signals from these interactions, as well as the ability of TSP1 to activate latent TGFβ and inhibit several proteases, may account for the complex responses of tumor and endothelium to TSP1 and have prevented a clear understanding of the role of TSP1 in the "angiogenic switch" [5]. Some of this complexity may be circumvented by using TSP1 peptides with defined activities. Based on antiproliferative peptides from the type 1 repeats of TSP1, stable analogs were designed that mimic the antitumor effects of the parent protein *in vivo* [1,2,45]. A D-inverse analog of this TSP1 sequence antagonized endothelial cell growth through its heparin-binding activity rather than by increasing cell adhesion or through activation of latent TGFβ [2]. The latter result was confirmed in this study, as the TGFβ activating-motif was not essential for inhibiting C6 glioma cell proliferation (Figure 1).

During the initial biodistribution studies, we found that the major fraction of TSP1-derived peptide P1 (>90% injected dose) was rapidly eliminated, with a residual small fraction circulating in the blood stream for hours, presumably, in a plasma protein-bound state. Some of the intravenously injected peptide was bound to neovasculature as determined by fluorescence microscopy (Figure 2) and amounted to overall tissue concentration of approximately 0.04% injected dose/g tumor within 1 hour after injection. This number, however, underestimates true endothelial concentration as it relates to the total tumor mass. The treatment of experimental tumors with TSP1-derived peptide markedly inhibited tumor growth. We observed that tumors treated with TSP1-derived peptide were significantly smaller (4–4.5 fold, $p < 0.001$) than tumors in animals that received control peptide. Although changes in tumor size were impressive, we found that the inhibition of tumor growth by TSP1-derived peptide was not associated with measurable changes in the relative blood volume fraction or vascular density (Table 2). However, the median area occupied by individual blood vessels in sectioned treated tumors (Figure 5) was significantly larger than in control peptide-treated tumors ($n = 300$, $p < 0.01$). In particular, a higher number of very dilated vessels (individual vessel area >2000 μm^2) was detected in control tumors. This may explain the somewhat lower vascularization of treated tumors, expressed as percentage of total area occupied by blood vessels (Table 2). A related observation was made before by magnetic susceptibility contrast MR imaging sensitive to blood vessel diameter [46]. The authors determined that in C6 glioma model, vessels are wider than their normal counterparts by 90%, on the average [46].

Therefore, histological corroboration of MR data confirms, in principle, that TSP1-derived peptide treatment of experimental glioma and gliosarcoma can lead to substantial inhibition of tumor growth that is associated only with very minor changes in relative blood volume or number of blood vessels in the tumor. This experimental observation is in agreement with the recent findings for other angiogenesis inhibitors, i.e., angiostatin and endostatin [47]. The observation of tumor growth retardation in the absence of concomitant changes in relative blood volume fraction could result from a direct antiproliferative effect of the TSP1-derived peptides on the glioma cells (Figure 1). Alternatively, tumor growth may be limited in both control and treated animals by the available vascular bed, growth of which is inhibited by the TSP1-derived peptide.

In conclusion, we have demonstrated that systemic administration of TSP1-derived peptides results in significant brain tumor growth retardation. This presumably occurs as a result of slower *de novo* blood vessel formation (antiangiogenesis) and synergistic direct antiproliferative effects on tumor cells. We have furthermore shown that previously developed *in vivo* MR imaging techniques can be used non-invasively to assess treatment efficacy of novel antiangiogenic drugs. Compared to traditional morphometric analysis, this tool is expected to be particularly useful in future clinical trials to evaluate antiangiogenic therapies.

References

[1] Guo N, Krutzsch H, Inman J, and Roberts D (1997). Thrombospondin 1 and type I repeat peptides of thrombospondin 1 specifically induce apoptosis of endothelial cells. *Cancer Res* **57**, 1735 – 1742.

[2] Guo H, Krutzsch H, Inman J, Shannon C, and Roberts D (1997). Antiproliferative and anti-tumor activities of D-reverse peptides from the second type-1 repeat of thrombospondin-1. *J Peptide Res* **50**, 210 – 217.

[3] Folkman J (1995). Angiogenesis in cancer, vascular, rheumatoid and other disease. *Nature Med* **1**, 27 – 31.

[4] Folkman J (1997). Angiogenesis and angiogenesis inhibition: an overview. *EXS* **79**, 1 – 8.

[5] Hanahan D, and Folkman J (1996). Patterns and emerging mechanisms of the angiogenic switch during tumorigenesis. *Cell* **86**, 353 – 364.

[6] Weidner N, Folkman J, Pozza F, Bevilacqua P, Allred E, Moore D, Meli S, and Gasparini G (1992). Tumor angiogenesis: a new significant and independent prognostic indicator in early-stage breast carcinoma. *J Natl Cancer Inst* **84**, 1875 – 1887.

[7] Abdulrauf S, Edvardsen K, Ho K, Yang X, Rock J, and Rosenblum M (1998). Vascular endothelial growth factor expression and vascular density as prognostic markers of survival in patients with low-grade astrocytoma. *J Neurosurgery* **88**, 513 – 520.

[8] O'Reilly MS, Holmgren L, Chen C, and Folkman J (1996). Angiostatin induces and sustains dormancy of human primary tumors in mice. *Nature Med* **2**, 689 – 692.

[9] O'Reilly MS, Boehm T, Shing Y, Fukai N, Vasios G, Lane WS, Flynn E, Birkhead JR, Olsen BR, and Folkman J (1997). Endostatin: an endogenous inhibitor of angiogenesis and tumor growth. *Cell* **88**, 277 – 285.

[10] Blumenthal RD, Sharkey RM, Haywood L, Natale AM, Wong GY, Siegel JA, Kennel SJ, and Goldenberg DM (1992). Targeted therapy of athymic mice bearing GW-39 human colonic cancer micrometastases with 131I-labeled monoclonal antibodies. *Cancer Res* **52**, 6036 – 6044.

[11] Molema G, Meijer DK, and de Leij LF (1998). Tumor vasculature targeted therapies: getting the players organized. *Biochem Pharmacol* **55**, 1939 – 1945.

[12] Dachs GU, Dougherty GJ, Stratford IJ, and Chaplin DJ (1997). Targeting gene therapy to cancer: a review. *Oncol Res* **9**, 313 – 325.

[13] Saleh M, Stacker SA, and Wilks AF (1996). Inhibition of growth of C6 glioma cells *in vivo* by expression of antisense vascular endothelial growth factor sequence. *Cancer Res* **56**, 393 – 401.

[14] Oku T, Tjuvajev JG, Miyagawa T, Sasajima T, Joshi A, Joshi R, Finn R, Claffey KP, and Blasberg RG (1998). Tumor growth modulation by sense and antisense vascular endothelial growth factor gene expression: effects on angiogenesis, vascular permeability, blood volume,

blood flow, fluorodeoxyglucose uptake, and proliferation of human melanoma intracerebral xenografts. *Cancer Res* **58**, 4185 – 4192.

[15] Im SA, Gomez-Manzano C, Fueyo J, Liu TJ, Ke LD, Kim JS, Lee HY, Steck PA, Kyritsis AP, and Yung WK (1999). Antiangiogenesis treatment for gliomas: transfer of antisense-vascular endothelial growth factor inhibits tumor growth *in vivo. Cancer Res* **59**, 895 – 900.

[16] Kirsch M, Strasser J, Allende R, Bello L, Zhang J, and Black PM (1998). Angiostatin suppresses malignant glioma growth *in vivo. Cancer Res* **58**, 4654 – 4659.

[17] Griscelli F, Li H, Bennaceur-Griscelli A, Soria J, Opolon P, Soria C, Perricaudet M, Yeh P, and Lu H (1998). Angiostatin gene transfer: inhibition of tumor growth *in vivo* by blockage of endothelial cell proliferation associated with a mitosis arrest. *Proc Natl Acad Sci USA* **95**, 6367 – 6372.

[18] Tanaka T, Cao Y, Folkman J, and Fine HA (1998). Viral vector-targeted antiangiogenic gene therapy utilizing an angiostatin complementary DNA. *Cancer Res* **58**, 3362 – 3369.

[19] Good D, Polverini P, Rastinejad F, Le Beau M, Lemosn R, Frazier W, and Bouck N (1990). A tumor suppressor-dependent inhibitor of angiogenesis is immunologically and functionally indistinguishable from a fragment of thrombospondin. *Proc Natl Acad Sci USA* **87**, 6624 – 6628.

[20] Taraboletti G, Roberts D, Liotta LA, and Giavazzi R (1990). Platelet thrombospondin modulates endothelial cell adhesion, motility, and growth: a potential angiogenesis regulatory factor. *J Cell Biol* **111**, 765 – 772.

[21] Murphy Ullrich J, and M H (1989). Thrombospondin modulates focal adhesions in endothelial cells. *J Cell Biol* **109**, 1309 – 1319.

[22] Vogel T, Guo N, Krutzsch H, Blake D, Hartman J, Mendelovitz S, Panet A, and Roberts D (1993). Modulation of endothelial cell proliferation, adhesion, and motility by recombinant heparin-binding domain and synthetic peptides from the type I repeats of thrombospondin. *J Cell Biochem* **53**, 74 – 84.

[23] Weinstat-Saslow D, Zabrenetzky V, VanHoutte K, Frazier W, Roberts D, and Steeg P (1994). Transfection of thrombospondin 1 complementary DNA into a human breast carcinoma cell line reduces primary tumor growth, metastatic potential, and angiogenesis. *Cancer Res* **54**, 6504 – 6511.

[24] Dameron KM, Volpert OV, Tainsky MA, and Bouck N (1994). Control of angiogenesis in fibroblasts by p53 regulation of thrombospondin-1. *Science* **265**, 1582 – 1584.

[25] Hsu SC, Volpert OV, Steck PA, Mikkelsen T, Polverini PJ, Rao S, Chou P, and Bouck NP (1996). Inhibition of angiogenesis in human glioblastomas by chromosome 10 induction of thrombospondin-1. *Cancer Res* **56**, 5684 – 5691.

[26] Sheibani N, and Frazier W (1995). Thrombospondin 1 expression in transformed endothelial cells restores a normal phenotype and suppresses their tumorigenesis. *Proc Natl Acad Sci USA* **92**, 6788 – 6792.

[27] Tolsma S, Volpert O, Good D, Frazier W, Polverini P, and Bouck N (1993). Peptides derived from two separate domains of the matrix protein thrombospondin-1 have antiangiogenic properties. *J Cell Biol* **122**, 497 – 511.

[28] Moore A, Marecos E, Simonova M, Weissleder R, and Bogdanov A, Jr. (1998). Novel gliosarcoma cell line expressing green fluorescent protein: a model for quantitative assessment of angiogenesis. *Microvasc Res* **56**, 145 – 153.

[29] Bogdanov A, Jr., Wright SC, Marecos EM, Bogdanova AV, Martin C, Petherick P, and Weissleder R (1997). A long-circulating co-polymer in "passive targeting" to solid tumors. *J Drug Targeting* **4**, 321 – 330.

[30] Bogdanov A, Jr., Weissleder R, Tsai E, Schaffer B, Bogdanova A, Nossiff N, Papisov M, and Brady T (1993) Tumor neovascularity imaging by contrast-enhanced MR angiography. 12th Annual Scientific Meeting Of Society of Magnetic Resonance in Medicine, New York, NY. p. 577.

[31] Bogdanov A, Jr., Weissleder R, Frank HW, Bogdanova AV, Nossif N, Schaffer BK, Tsai E, Papisov MI, and Brady TJ (1993). A new macromolecule as a contrast agent for MR angiography: preparation, properties, and animal studies. *Radiology* **187**, 701 – 706.

[32] Weissleder R, Cheng H, Marecos E, Kwon K, and Bogdanov A (1998). Mapping of tumor vascular and interstitial volume fractions non invasively *in vivo. Eur J Cancer* **34**, 1444 – 1454.

[33] Hendrick RE, and Haacke EM (1993). Basic physics of MR contrast agents and maximization of image contrast. *JMRI* **3**, 137 – 148.

[34] Donahue KM, Weisskoff RM, Chesler D, Kwong K, Bogdanov AA, Mandeville JB, and Rosen BR (1996). Improving MR quantification of regional blood volume with intravascular T1 contrast agents: accuracy, precision, and water exchange. *Magn Reson Med* **36**, 858 – 867.

[35] Smith K, Hill S, Begg A, and Denekamp J (1988). Validation of the fluorescent dye Hoechst 33342 as a vascular space marker in tumors. *Br J Cancer* **57**, 247 – 253.

[36] Vogel A (1965). Intratumoral vascular changes with increased size of a mammary adenocarcinoma: new method and results. *J Natl Cancer Inst* **34**, 571 – 578.

[37] Fallowfield M (1989). Vascular volume in B16 allografts and human melanoma xenografts estimated by means of Hoechst 33342. *J Pathol* **157**, 249 – 252.

[38] Samoto K, Ikezaki K, Ono M, Shono T, Kohno K, and Kuwano M (1995). Expression of vascular endothelial growth factor and its possible relation with neovascularization in human brain tumors. *Cancer Res* **55**, 1189 –1193.

[39] Hansen S, Grabau D, Bak M, Rose C, and Sorensen F (1998). Estimating intratumoral microvessel density by different methods to determine angiogenesis in breast cancer: intra- and interobserver variability. Proceedings of AACR Symposium: Angiogenesis and Cancer, Orlando, FL. A-47.

[40] Parangi S, O'Reilly M, Christofori G, Holmgren L, Grosfeld J, Folkman J, and Hanahan D (1996). Antiangiogenic therapy of transgenic mice impairs de novo tumor growth. *Proc Natl Acad Sci USA* **93**, 2002 – 2007.

[41] Boehm T, Folkman J, Browder T, and O'Reilly MS (1997). Antiangiogenic therapy of experimental cancer does not induce acquired drug resistance. *Nature* **390**, 404 – 407.

[42] Roberts DD (1996). Regulation of tumor growth and metastasis by thrombospondin-1. [69 refs]. *FASEB J* **10**, 1183 – 1191.

[43] Tuszynski GP, and Nicosia RF (1996). The role of thrombospondin-1 in tumor progression and angiogenesis. *Bioessays* **18**, 71 – 76.

[44] Qian X, and Tuszynski GP (1996). Expression of thrombospondin-1 in cancer: a role in tumor progression. *Proc Soc Exp Biol Med* **212**, 199 – 207.

[45] Dawson D, Volpert O, Pearce F, Schneider A, Silverstein R, Henkin J, and Bouck N (1999). Three distinct D-amino acid substitutions confer potent antiangiogenic activity on an inactive peptide derived from a thrombospondin type 1 peptide. *Mol Pharmacol* **55**, 332 – 338.

[46] Dennie J, Mandeville J, Boxerman J, Packard S, Rosen B, and Weisskoff R (1998). NMR imaging of changes in vascular morphology due to tumor angiogenesis. *Magn Reson Med* **40**, 793 – 799.

[47] Bergers G, Javaherian K, Lo K, Folkman J, and Hanahan D (1999). Effects of angiogenesis inhibitors on multistage carcinogenesis in mice. *Science* **284**, 808 – 812.